

Micro-Facies Analysis and Geochemistry of Shaley-Banded Iron Formations (S-Bifs) from Late-Archaean Kushtagi-Hungund Schist Belt (KHSB), Karnataka, South Indian Shield (SIS)

Arunava Sen¹, Soumik Mukhopadhyay¹, Pradip Samanta², Anisha Ghosh¹, and Dipak Pal¹

¹Jadavpur University

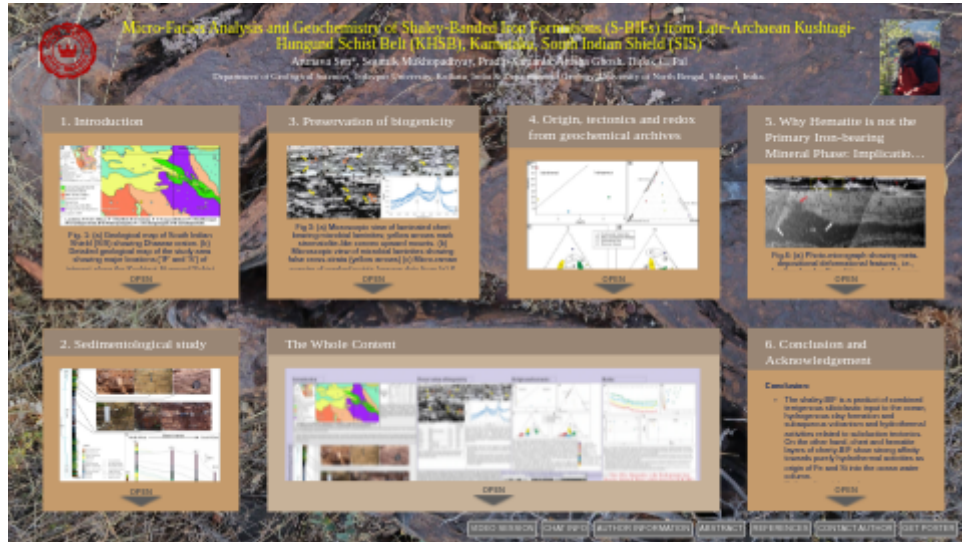
²University of North Bengal

November 24, 2022

Abstract

Present work deals with paleogeographic reconstruction through sequence modelling, facies and micro-facies analysis and biogeochemical investigations of late Archaean Banded Iron Formations (BIFs) from Kushtagi-Hungund Schist Belt (KHSB) of Eastern Dharwar Craton (EDC), South Indian Shield (SIS). This comparatively less metamorphosed schist belt of EDC is correlated to the Bababudan Group of Dharwar Supergroup, Western Dharwar Craton (WDC). The lower and upper age constraints have been established from dating of 3.4-3.1 Ga old underlying Sargur Group and TTG gneisses, and 2.5 Ga old younger granites, intruding the KHSB metasediments, respectively. Further, metavolcanics intercalating with the metasediments of KHSB have been dated at 2750-2670 Ma. In this work, special emphasis has been given to the shaley-BIFs of this schist belt which is comprised of thin (few millimeters to a maximum of 1.2-1.5 cm thick) alternating units of iron rich shale, chert and hematite. Facies analysis and sequence model reveal deep water, offshore paleogeography, where proximal outer shelf is dominated by shaley siliciclastics and distal outer shelf and further deep oceanic succession is occupied by chert-hematite-dominated chemogenic sediment suits. Micro-facies analysis of the shaley-BIFs elucidated the interaction between chemogenic and deep water siliciclastic and volcanoclastic shaley sediments within micro domains. Primary chert layers contain several permineralized structures associated with carbonaceous matters. Recent RAMAN spectrometric analysis (compared to previous data in provided figure) and Carbon-isotopic values ($\delta^{13}C$ values ranging from -22.08 to -30.84 (ranging from 0.03 to 0.14 ‰) from cherts and shales indicate preservation of Archean biogenic remnants. Recent elemental (major and trace) and oxygen isotopic data, associated with the micro-facies systematics of shale-chert-iron oxide units, have been compared to previously published geochemical data sets derived from KHSB and other BIFs of SIS to provide important clues and new insights regarding late Archean ocean water chemistry, redox state, paleoclimate and control of tectonics and provenance on sedimentation pattern, prior to Great Oxygenation Event (GOE).

Micro-Facies Analysis and Geochemistry of Shaley-Banded Iron Formations (S-BIFs) from Late-Archaean Kushtagi-Hungund Schist Belt (KHSB), Karnataka, South Indian Shield (SIS)



Arunava Sen*, Soumik Mukhopadhyay, Pradip Samanta, Anisha Ghosh, Dipak C. Pal

Department of Geological Sciences, Jadavpur University, Kolkata, India & Department of Geology, University of North Bengal, Siliguri, India.



PRESENTED AT:



1. INTRODUCTION

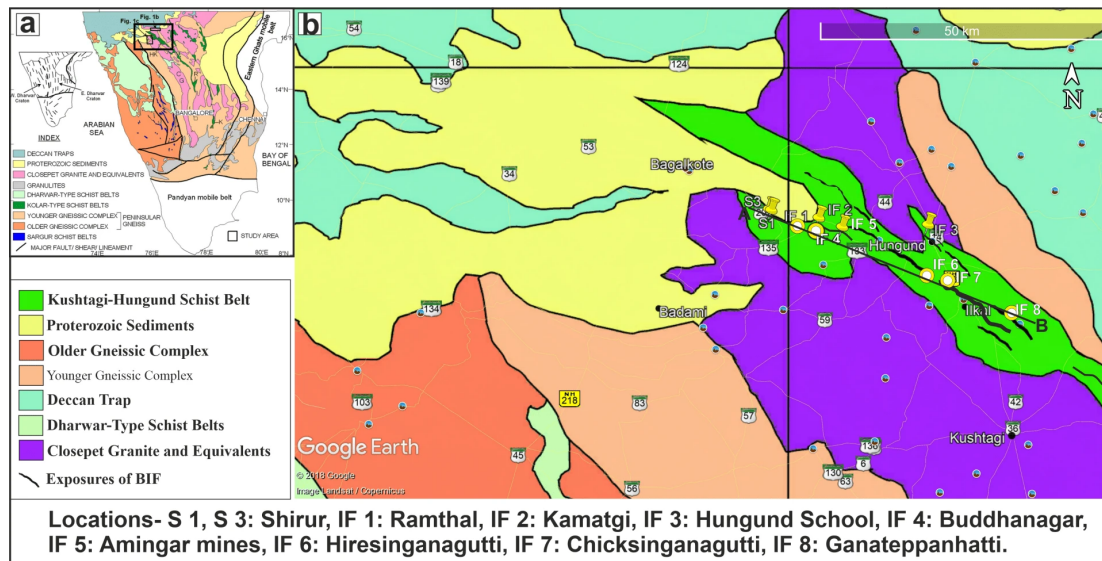


Fig- 1: (a) Geological map of South Indian Shield (SIS) showing Dharwar craton. (b) Detailed geological map of the study area showing major locations ('IF' and 'S') of interest along the Kushtagi-Hungund Schist Belt (KHSB).

- Kushtagi-Hungund Greenstone belt within the Eastern Dharwar Craton (EDC) stretches from Kushtagi to Kilarhatti and Ilkal and it is about 100km of length and 8km wide at maximum stretch near Hungund and Kushtagi (Naqvi et al., 2006). Upto the shear zone between EDC and Western Dharwar Craton WDC the major lithology comprises of high-Mg tholeiitic pillow basalts, massive metabasalts and Banded Hematitequartz interbedded with ferruginous shale to silt and sometimes with acid and basic volcanics (Khan and Naqvi, 1996; Naqvi, 2006).

Ramagiri-Hungund GSB	Lithology	Method	Age	Authors
	Pyroclastics, Central "prong" in the schist belt	Zircon, TIMS	2707±18 Ma	Balakrishnan et al. (1999)
	Chenna migmatitic gneisses	Sphene	2545±1Ma	Balakrishnan et al. (1999)
	Chenna migmatitic gneisses	Zircon	2650±8Ma	Balakrishnan et al. (1999)
	Central granitoid Ramagiri	Zircon	2614±4Ma	Balakrishnan et al. (1999)
	Central granitoid Ramagiri	Sphene	2613±7Ma	Balakrishnan et al. (1999)
	W. Gangam plutonic complex	Zircon	2528±1Ma	Balakrishnan et al. (1999)
	Post kinematic granite	Sphene	2468±4Ma	Balakrishnan et al. (1999)
	Metabasalt	Pb-Pb	2746±64Ma	Zachariah et al. (1995)
Old continental crust and EW diabase dyke	Sm-Nd	2454±100Ma	Zachariah et al. (1995)	

Table 1: Geochronological data showing the age of different basement components, intrusives, pyroclastics, volcanics and metabasalts of the Ramgiri-Hungund Super Belt (RHSB). KHSB being the northern part of RHSB, metasediments of this greenstone belt lie between an age constraint of 2.6-2.7 Ga.

2. SEDIMENTOLOGICAL STUDY

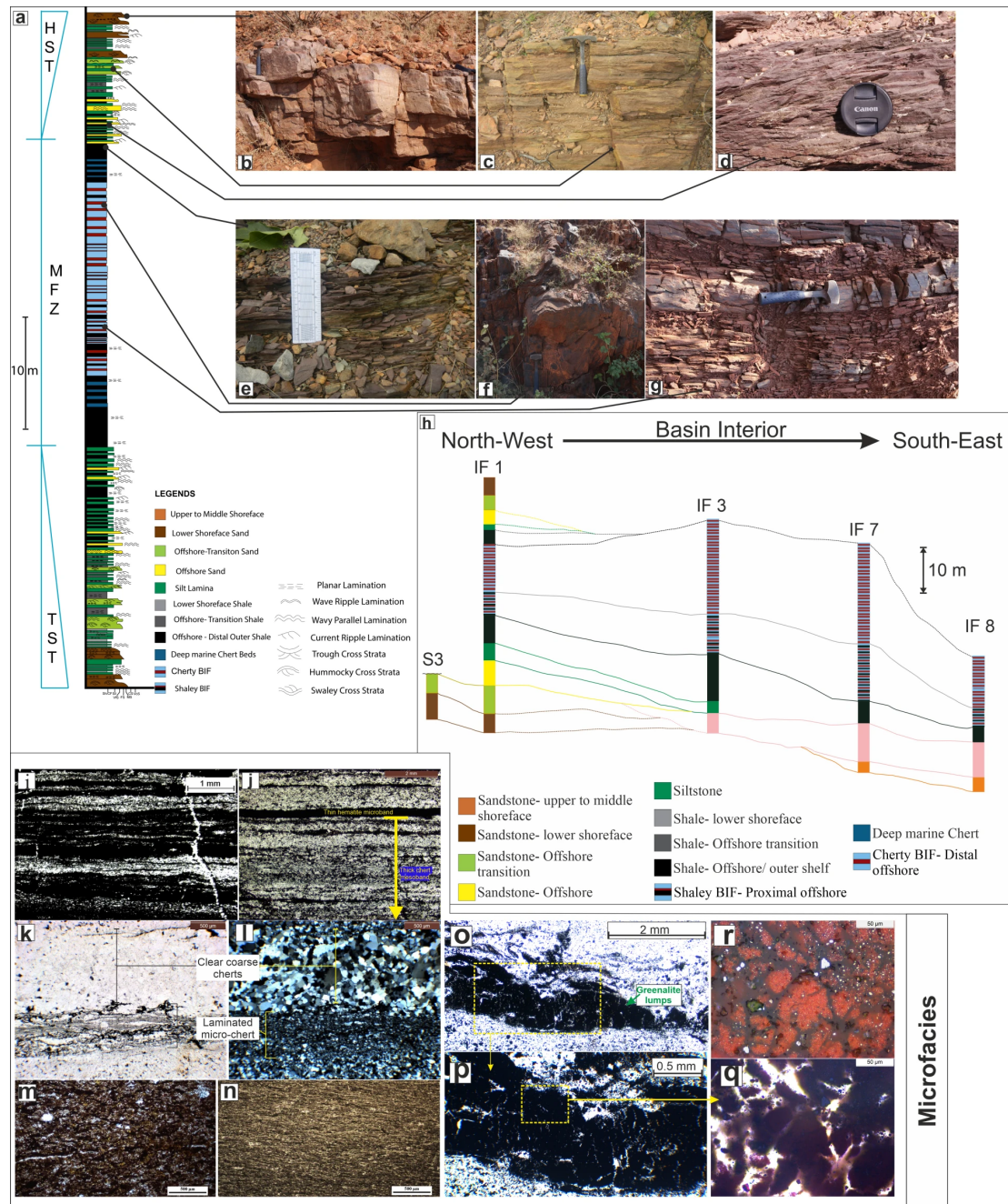


Fig- 2: (a) Lithological log of an ideal succession from Ramthal area (Location- IF-, Fig- 1) showing facies and facies associations and the sequence development pattern. The succession shows an initial fining upward trend and then a coarsening upward trend with a Maximum Flooding Zone (MFZ), devoid of siliciclastic terrigenous sediments and demarcated with dark-grey to black shales and chemically precipitated chert and iron oxide rich components of BIF. Facies: (b) Hummocky cross-stratified medium grained sandstone from lower shoreface; (c) Planar laminated fine grained sandstone intercalated with ripple laminated siltstone from offshore transition; (d) Ripple laminated sand-silt-stone intercalation with occasional grey shale from offshore; (e) Planar laminated dark grey shale; (f) Thick chert-iron oxide intercalation of cherty BIF from distal offshore and (g) Thinly intercalated chert-iron oxide unit interbedded with grey and black shale from distal offshore; (h) Synthetic fence correlating major successions along the studied portion (A-B traverse marked in Fig-1b) of KHSB. Microfacies: Petrographic images of (i) Thin alternations of chert and haematite microbands; (j) Thick alternations of chert mesobands containing discrete iron oxide microlaminations; (k & l) Plane polarised and crossed polarised view of clear coarse grained (80-100 microns grain diameter) alternating with laminated microgranular (<10-35 microns grain diameter) grey chert respectively; (m) Plane polarised view of ferruginous black shale; (n) Iron rich grey shale under reflected light (PPL); (o) Plane polarised photo-montage of greenalite layer showing polygonal shrinkage cracks; (p) Magnified view of (o); (q) Magnified view of the dotted yellow box from (p) showing anhedral to

subhedral greenalite lumps and shrinkage crack network filled with chert surrounding the Fe-silicate masses;
(r)Plane polarised view of (q) showing greenalite lumps, chert filled crack network and euhedral haematite phases within the crack network.

- State-of-art facies study and sequence architectural analysis on KHSB metasediments have helped in interpreting depositional environment and reconstruction of paleogeography. The study shows that sedimentation took place within an Archean marine depocentre and the depositional realm transits from a sand dominated shallow shoreface paleogeography to offshore deep marine regime dominated with dark grey-black shales and chemogenic chert-iron oxide assemblages.
- Sequence stratigraphic investigation on several successions reveals an initial fining upward sedimentation trend associated with the gradually deepening upward Transgressive System Tract (TST) at the bottom part of the successions and coarsening upward trend associated with gradually shallowing upward Highstand System Tract (HST) at the upper part of the successions, with a condensed zone filled with black shales gradually transiting to shaley BIF to cherty BIF demarcating the deepest portion of submarine depository, i.e. the Maximum Flooding Zone (MFZ).
- The deepest portion of the depocentre show a transition from siliciclastic black shales to allochemically deposited shaley BIFs to purely chemogenic cherty BIFs. This suggests a gradual cease in siliciclastic supply with the deepening of the paleogeography and dominance of chemical precipitation within an undisturbed deep marine water column.
- Correlation of synthetic lithosections demonstrates a shallower paleogeography to the north-west end of the greenstone belt and a deeper paleogeography to the south-east end.
- Detailed microfacies analysis has revealed presence of microgranular laminated silica and Fe-silicate (greenalite) like components within this apparently chert-iron oxide dominated BIF.
- The crack network within the greenalite layers indicate meta-depositional and syn-compactional crack forming within these Fe-silicate layers due to fluid escape and consequent shrinkage. The presence of silica (chert) and euhedral iron oxide phases surrounding the greenalite lumps and within the cracks might suggests post depositional breakdown of Fe-silicate phases to silica and iron oxides/hydroxides.

3. PRESERVATION OF BIOGENICITY

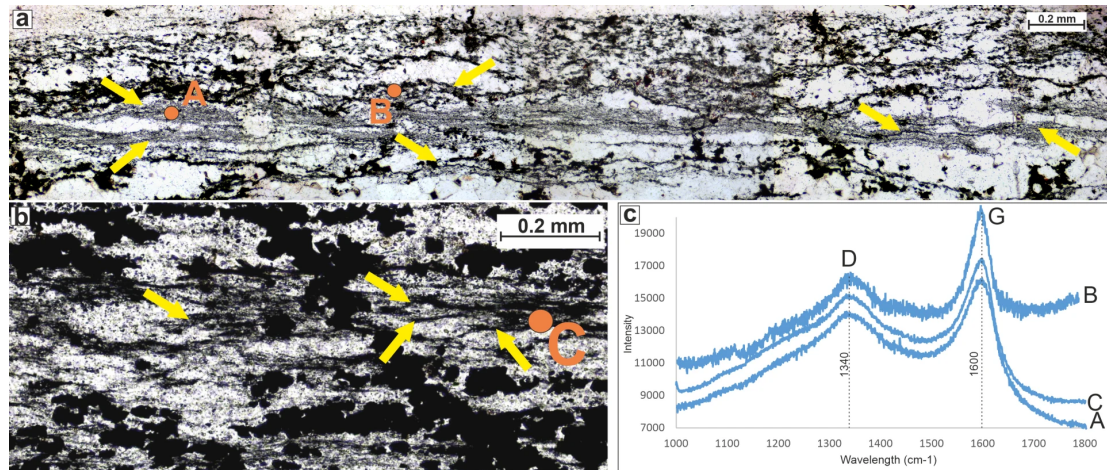


Fig 3: (a) Microscopic view of laminated chert bearing microbial laminites; yellow arrows mark stromatolite-like convex upward mounts. (b) Microscopic view of microbial laminites showing false cross-strata (yellow arrows) (c) Micro-Raman spectra of marked points (orange dots from (a) & (b)) showing D & G peak defining nano-disordered carbon and graphitic inclusions within chert matrix hosted laminites - Probable presence of kerogenous organic matter.

Sample Name	Lithology	TOC (%)	Corrected d ¹³ C values
BF-7A	Shale	0.22	-27.88
BF-6	Silt-Shale intercalation	0.13	-30.84
KRM-15	Shale	0.14	-22.21
KRM-8	Shale	0.26	-26.41
KRM-5	Shale	0.14	-24.08
KRM-10	Shale	0.19	-26.51
KRM-16	Laminated Chert	0.48	-31.38
KAG-2	Greenalite layer	0.28	-29.62
KRM-9	Dusty Chert with Greenalite	0.37	-32.27

Table 2: Total organic carbon (TOC) content and corresponding d¹³CVPDB values of laminated chert, greenalite bearing layers and associated shales indicating preservation of biogenic matter within these late Archean oceanic sediments.

- The laminated cherts bear several signatures of microbially induced primary structures, that resembles stromatolite and microbial laminites previously reported from other Archean Iron Formations.
- MicroRaman spectrometry and carbon isotopic studies confirm the biogenicity of these laminated chert, greenalite (Fe-silicate) bearing layers and dark grey shales. The presence of kerogenous matter within laminated and Fe-silicate microfacies bears grave significance in enlightening biogeochemical implications related to Archean biosphere.

4. ORIGIN, TECTONICS AND REDOX FROM GEOCHEMICAL ARCHIVES

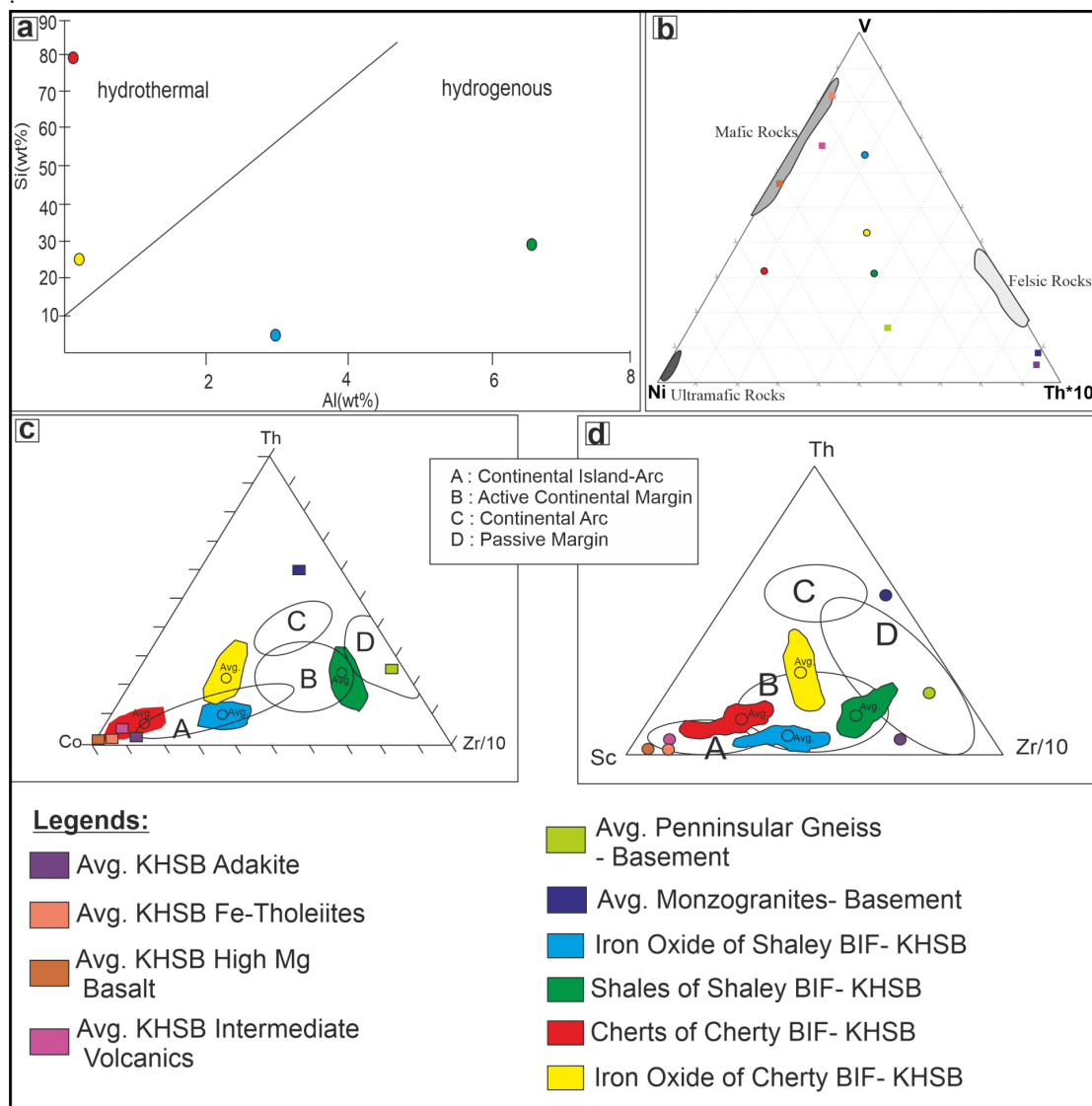


Fig 4: (a) Si vs Al plot showing dominantly hydrothermal affinity for cherty BIF components and hydrogenous affinity of shaley BIF components. (b) V- Ni-Th triangular diagram indicating trace element contribution from mafic and ultramafic provenance dominant in iron and silica rich components of BIFs, whereas shaley BIF relatively more inclined towards felsic provenance. (c) Th-Co-Zr triangular plot indicating Island-arc tectonic setting for most of the cherty and shaley BIFs except for shale rich ones, which indicates active continental margin. (d) Th-Sc-Zr triangular plot indicating Active continental margin for all type of BIFs. [Data source: Chert (n=16) and iron oxide (n=6) of cherty BIF, KHSB (Khan, 1993); shale (n=12) and iron oxide (n=7) of shaley BIF (Khan, 1993); adakites (n=15), intermediate volcanics (n=10), high Mg-basalts (n=12), Fe-tholeiites (n=2) of KHSB (Naqvi et al., 2006); Peninsular gneiss (n=6), monzogranites (n=10) from basement (Dey et al., 2012).]

- The silica and iron rich components of the studied iron formation show affinity towards hydrothermal processes influencing their formation and subaqueous precipitation and a correlation with mafic volcanics. The tectonic setup might have been a convergent tectonic boundary associated with syn-sedimentary volcanisms. The terrigenous input, on the other hand, is recorded within shale dominated portions of the BIF.

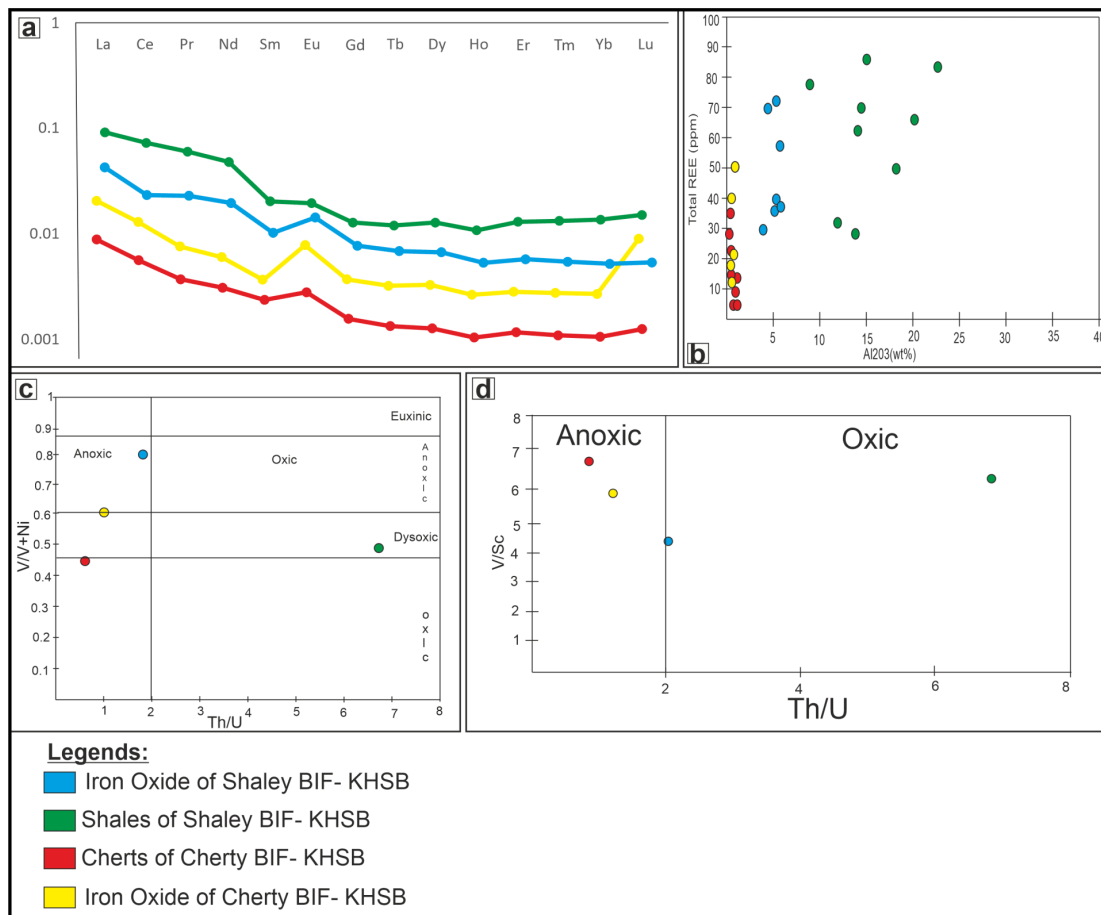


Fig 5: (a) Normalized data plot of BIFs showing no significant Ce anomaly and prominent Eu anomaly indicating hydrothermal influence. (b) Al_2O_3 vs total REE plot indicating trivial detrital input for all BIFs except shale rich BIFs. (c) Th/U vs V/(V+Ni) plot indicating overall anoxic paleoredox condition. (d) Th/U vs V/Sc plot indicating anoxic paleo-redox condition for cherty BIFs and iron rich shaley BIFs and oxic paleo-redox condition for shale rich shaley BIFs.

- The geochemical data indicates that the deeper most siliciclastic components were sedimented within an oxic to dysoxic realm where the chemogenic silica and iron oxide components of both shaley and cherty BIFs were precipitated within an anoxic water column devoid of siliciclastic input and free oxygen.
- The deposition of silica and iron oxide components is thus inclined towards a deep marine anoxic reservoir of Si and Fe where biogeochemical processes and ocean water chemistry (Eh, pH & Temperature) might have interplayed as pivotal boundary conditions behind the origin of these pre-GOE chemical sediments.
- Evidence behind the anoxic depositional realm as the sink for aqueous Si & Fe does not supports the formation of iron oxide (haematite) phases as the primary iron bearing mineral phase in these late Archean BIFs.

Then Why Hematite is the Predominant Iron Bearing Mineral Phase within these Pre-GOE BIFs ???

5. WHY HEMATITE IS NOT THE PRIMARY IRON-BEARING MINERAL PHASE: IMPLICATIONS BEHIND FE-SILICATE (GREENALITE) PRECIPITATION

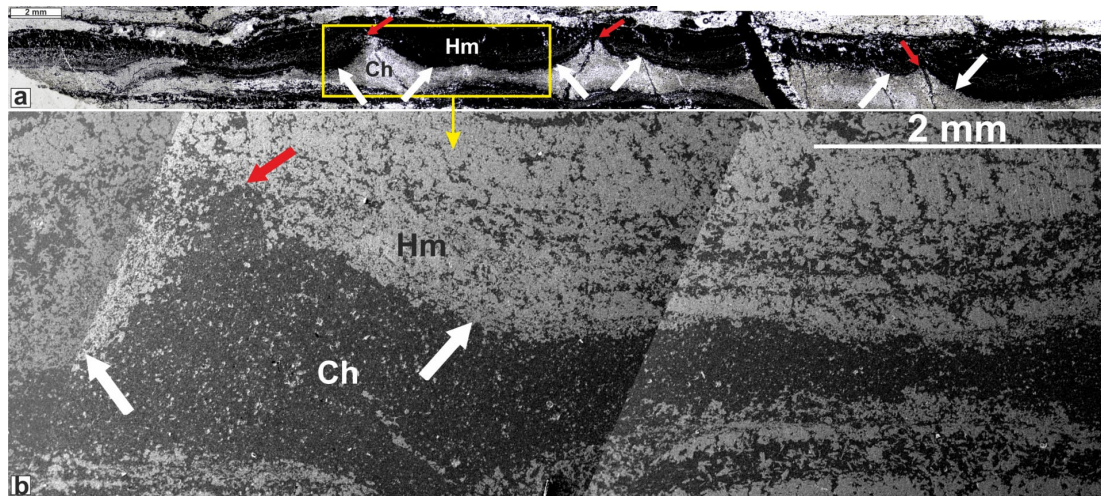


Fig-6: (a) Photo-micrograph showing meta-depositional deformational features, i.e., loading (marked by white arrows) of denser hematite bearing layer into the underlying chert (silica) layer and fluid escape structures (marked by red arrows) formed due to loading and compaction within the hematite bearing layer. (b) SEM-SE image of the yellow rectangle-marked portion of (a). Ch: chert; Hm: hematite.

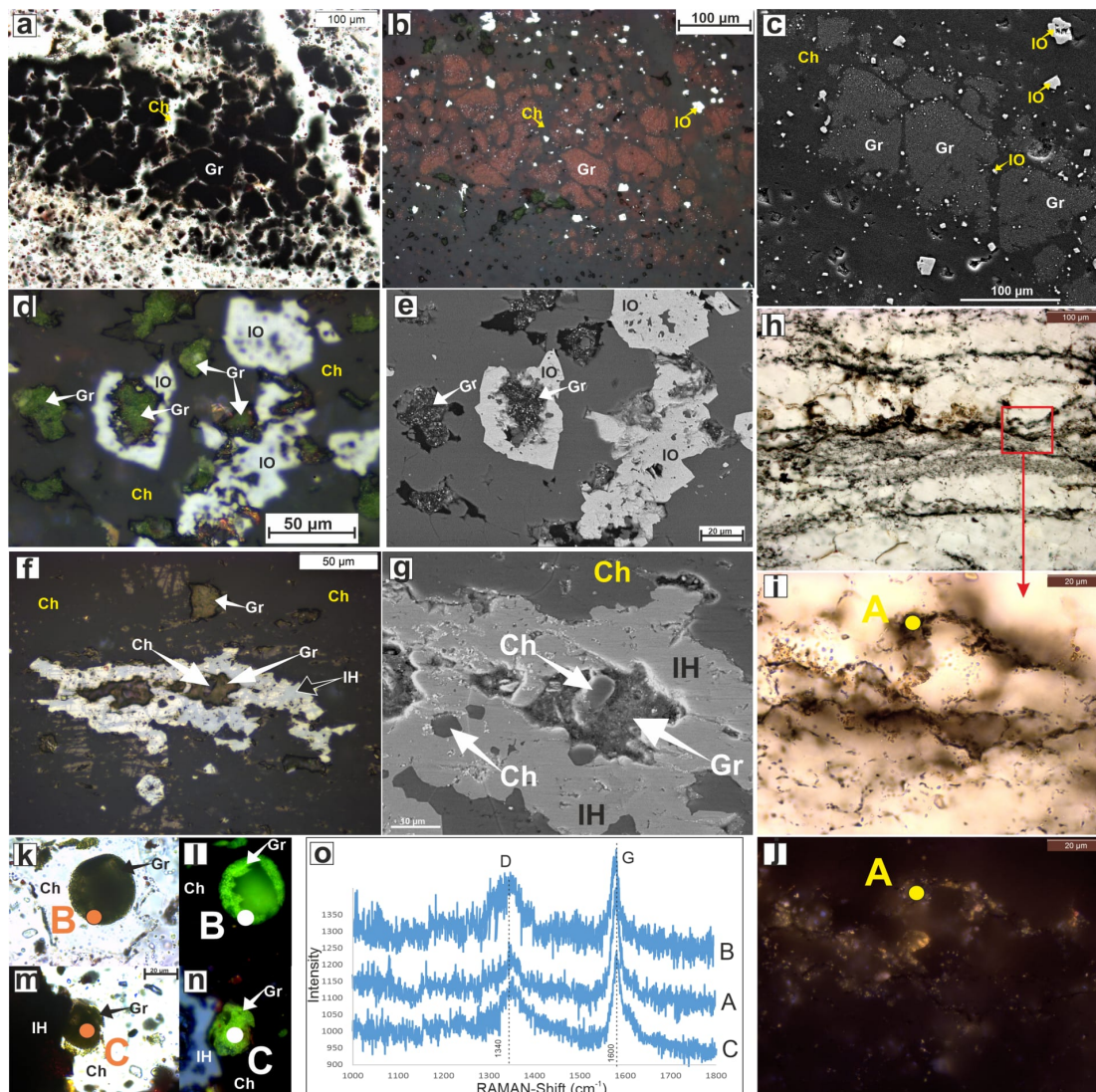
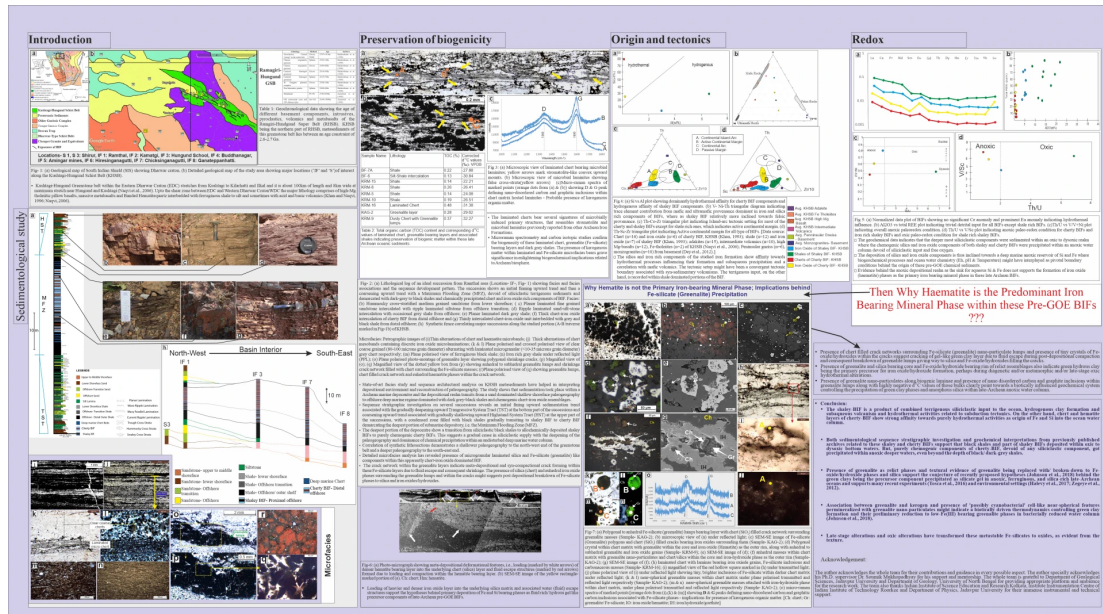


Fig-7: (a) Polygonal to anhedral Fe-silicate (greenalite) lumps bearing layer with chert (SiO₂) filled crack network surrounding greenalite masses (Sample- KAG-2); (b) microscopic view of (a) under reflected light; (c) SEM-SE image of Fe-silicate (Greenalite) polygons and chert (SiO₂) filled cracks bearing iron oxides surrounding them (Sample- KAG-2); (d) Polygonal crystal within chert matrix with greenalite within the core and iron oxide (Hematite) as the outer rim, along with anhedral to subhedral greenalite and iron oxide grains (Sample- KRM-9); (e) SEM-SE image of (d); (f) anhedral masses within chert matrix with greenalite nano-particulates and chert/silica within the core and iron-hydroxide phase as the outer rim (Sample- KAG-2); (g) SEM-SE image of (f); (h) laminated chert with laminae bearing iron oxide grains, Fe-silicate inclusions and carbonaceous masses (Sample- KRM-16); (i) magnified view of the red hollow square marked in (h) under transmitted light; (j) plane polarized view of (i) under reflected light showing tiny, brighter inclusions of Fe-silicate within darker chert matrix under reflected light; (k & l) near-spherical greenalite masses within chert matrix under plane polarised transmitted and reflected light respectively (Sample- KAG-2); (m & n) near-spherical greenalite masses attached with iron-hydroxide phase within chert matrix, under plane polarised transmitted and reflected light respectively (Sample- KAG-2); (o) micro-Raman spectra of marked points [orange dots from (i),(k) & (m)] showing D & G peaks defining nano-disordered carbon and graphitic carbon inclusions associated with Fe-silicate phases - implications for presence of kerogenous organic matter. [Ch: chert; Gr: greenalite/ Fe-silicate; IO: iron oxide/hematite; IH: iron hydroxide/goethite]

- Loading of heavier and denser iron oxide layer into the underlying silica matrix and associated water (fluid) escape structures support the hypotheses behind primary deposition of Fe and Si bearing phases as fluid rich/ hydrous gel like precursor components of late-Archean pre-GOE BIFs.
- Presence of chert filled crack networks surrounding Fe-silicate (greenalite) nano-particulate lumps and presence of tiny crystals of Fe-oxide/hydroxides within the cracks suggest cracking of gel-like green clay layer due to fluid escape during post-depositional compaction and consequent breakdown of greenalite lumps giving way to silica and Fe-oxide/hydroxides filling the cracks.
- Presence of greenalite and silica bearing core and Fe-oxide/hydroxide bearing rim of relict assemblages also indicate green hydrous clay being the primary precursor for iron oxide/hydroxide formation, perhaps during diagenetic and/or metamorphic and/or late-stage oxic hydrothermal alterations.
- Presence of greenalite nano-particulates along biogenic laminae and presence of nano disordered carbon and graphite inclusions within greenalite lumps along with highly negative $\delta^{13}\text{C}$ values of those bulks clearly point towards a biotically influenced geochemical system controlling the precipitation of green clay phases and amorphous silica within late-Archean anoxic water column.

THE WHOLE CONTENT



6. CONCLUSION AND ACKNOWLEDGEMENT

Conclusion:

- The shaley-BIF is a product of combined terrigenous siliciclastic input to the ocean, hydrogenous clay formation and subaqueous volcanism and hydrothermal activities related to subduction tectonics. On the other hand, chert and hematite layers of cherty-BIF show strong affinity towards purely hydrothermal activities as origin of Fe and Si into the ocean water column.
- Both sedimentological sequence stratigraphic investigation and geochemical interpretations from previously published archives related to these shaley and cherty BIFs support that black shales and part of shaley BIFs deposited within oxic to dysoxic bottom waters. But, purely chemogenic components of cherty-BIF, devoid of any siliciclastic component, got precipitated within anoxic deeper waters, even beyond the depth of black/ dark-grey shales.
- Presence of greenalite as relict phases and textural evidence of greenalite being replaced with/ broken-down to Fe-oxide/hydroxide phases and silica support the conjecture of recently proposed hypotheses (Johnson et al., 2018) behind the green clays being the precursor component precipitated as silicate gel in anoxic, ferruginous, and silica-rich late-Archean oceans and supports many recent experiments (Tosca et al., 2016) and environmental settings (Halevy et al., 2017; Zegeye et al., 2012).
- Association between greenalite and kerogen and presence of 'possibly cyanobacterial' cell-like near-spherical features permineralized with greenalite nano-particulates might indicate a biotically driven thermodynamics controlling green clay formation and their preliminary reduction to low-Fe (III) bearing greenalite phases in bacterially reduced water column (Johnson et al., 2018).
- Late-stage alterations and oxic alterations have transformed these metastable Fe-silicates to oxides, as evident from the texture.

Acknowledgement:

The author acknowledges the whole team for their contributions and guidance in every possible aspect. The whole team is grateful to Department of Geological Sciences, Jadavpur University and Department of Geology, University of North Bengal for providing appropriate platform and ambience for the research work. The team also thanks Indian Institute of Science Education and Research Kolkata, Institute Instrumentation Centre of Indian Institute of Technology Roorkee and Department of Physics, Jadavpur University for their immense instrumental and technical support.

AUTHOR INFORMATION

Arunava Sen

Pursuing Ph.D. as DAE-BRNS-Senior Research Fellow (SRF) in Jadavpur University, Kolkata- 700032, India, under the supervision of Dr. Soumik Mukhopadhyay, Associate Prof., Dept. of Geological Sciences, Jadavpur University.

Research Domain:

Sedimentology and Paleo-geobiology of Precambrian Time; Paleoclimatology, Sediemntary Geochemistry.

ABSTRACT

Abstract Text:

Present work delivers major focus on development of paleogeographic reconstruction through sequence modelling, facies and micro-facies analysis and bio-geochemical investigations of late Archaean BIFs from Kushtagi-Hungund Schist Belt (KHSB) of Eastern Dharwar Craton (EDC), Karnataka, South Indian Shield. This comparatively younger schist belt of EDC is correlated to the Bababudan Group of Dharwar Supergroup, Western Dharwar Craton (WDC). The lower and upper age constraints have been established from dating of 3.4-3.1 Ga old underlying Sargur Group and TTG gneisses, and 2.5 Ga old younger granites, intruding the KHSB metasediments, respectively. Further, metavolcanics intercalating with the metasediments of KHSB have been dated at 2750-2670 Ma. In this work, special emphasis has been given to the shaley-BIFs (S-BIFs) of this schist belt which is comprised of thin (few millimetres to a maximum of 1.2-1.5 cm thick) alternating units of iron rich shale, chert and hematite. Facies analysis and sequence model reveal deep water, offshore paleogeography, where proximal outer shelf is dominated by shaley siliciclastics and distal outer shelf and further deep oceanic succession is occupied by chert-hematite-dominated chemogenic sediment suits. Micro-facies analysis of the shaley-BIFs elucidated the interaction between chemogenic and deep water siliciclastic and volcanoclastic shaley sediments within micro domains. Primary chert layers contain several permineralized structures associated with carbonaceous matters. RAMAN spectrometric analysis and Carbon-isotopic values ($\delta^{13}C$ values ranging from -22.08 to -30.84 ‰ -VPDB, n= 12) of Total Organic Carbon (TOC) (ranging from 0.03 to 0.14 %) from cherts and shales indicate preservation of Archean biogenic remnants. Also, oxygen isotopic studies of cherts associated with micro-facies along with major and trace element geochemistry of chert and shales provide important clues in deciphering Archean ocean water chemistry, redox state, paleoclimate and control of tectonics and provenance on sedimentation pattern, as well as the extent of post-diagenetic/ metamorphic modifications of isotopic and elemental compositions.

REFERENCES

- Baioumy, H., Lehmann, B., Salim, A.M.A., Al-Kahtany, K. and El-Sorogy, A., 2020. Geochemical characteristics of black shales from Triassic turbidites, Peninsular Malaysia: Implications for their origin and tectonic setting. *Marine and Petroleum Geology*, 113, p.104137.
- Balakrishnan, S., Rajamani, V. and Hanson, G.N., 1999. U-Pb ages for zircon and titanite from the Ramagiri area, southern India: Evidence for accretionary origin of the eastern Dharwar craton during the late Archean. *The Journal of geology*, 107(1), pp.69-86.
- Condie, K.C., 1993. Chemical composition and evolution of the upper continental crust: contrasting results from surface samples and shales. *Chemical geology*, 104(1-4), pp.1-37.
- Friese, A., Bauer, K., Glombitza, C., Ordoñez, L., Ariztegui, D., Heuer, V.B., Vuillemin, A., Henny, C., Nomosatryo, S., Simister, R. and Wagner, D., 2021. Organic matter mineralization in modern and ancient ferruginous sediments. *Nature communications*, 12(1), pp.1-9.
- Gourcerol, B., Thurston, P.C., Kontak, D.J. and Côté-Mantha, O., 2015. Interpretations and implications of LA ICP-MS analysis of chert for the origin of geochemical signatures in banded iron formations (BIFs) from the Meadowbank gold deposit, Western Churchill Province, Nunavut. *Chemical Geology*, 410, pp.89-107.
- Halevy, I., Alesker, M., Schuster, E.M., Popovitz-Biro, R. and Feldman, Y., 2017. A key role for green rust in the Precambrian oceans and the genesis of iron formations. *Nature Geoscience*, 10(2), pp.135-139.
- Jayananda, M., Aadhiseshan, K.R., Kusiak, M.A., Wilde, S.A., Sekhamo, K.U., Guitreau, M., Santosh, M. and Gireesh, R.V., 2020. Multi-stage crustal growth and Neoproterozoic geodynamics in the Eastern Dharwar Craton, southern India. *Gondwana Research*, 78, pp.228-260.
- Johnson, J.E., Muhling, J.R., Cosmidis, J., Rasmussen, B. and Templeton, A.S., 2018. Low-Fe (III) greenalite was a primary mineral from Neoproterozoic Oceans. *Geophysical Research Letters*, 45(7), pp.3182-3192.
- Kato, Y., 2005. Rare-earth elements in Precambrian banded iron formations: secular changes of Ce and Eu anomalies and evolution of atmospheric oxygen. *Evolution of Early Earth's Atmosphere, Hydrosphere and Biosphere-Constraints from Ore Deposits*.
- Khan, R.M.K. and Naqvi, S.M., 1996. Geology, geochemistry and genesis of BIF of Kushtagi schist belt, Archaean Dharwar Craton, India. *Mineralium Deposita*, 31(1-2), pp.123-133.
- Khan, R.M.K., 1993. Geology, geochemistry and Palaeoenvironment of Deposition of Banded Iron Formation of the Kushtagi schist belt, Karnataka Nucleus, India. Unpublished PhD thesis, Aligarh Muslim University, Aligarh.
- Khan, R.M.K., Sharma, S.D., Patil, D.J. and Naqvi, S.M., 1996. Trace, rare-earth element, and oxygen isotopic systematics for the genesis of banded iron-formations: Evidence from Kushtagi schist belt, Archaean Dharwar Craton, India. *Geochimica et Cosmochimica Acta*, 60(17), pp.3285-3294.
- McDonough, W.F. and Sun, S.S., 1995. The composition of the Earth. *Chemical geology*, 120(3-4), pp.223-253.
- Schad, M., Halama, M., Bishop, B., Konhauser, K.O. and Kappler, A., 2019. Temperature fluctuations in the Archean ocean as trigger for varve-like deposition of iron and silica minerals in banded iron formations. *Geochimica et Cosmochimica Acta*, 265, pp.386-412.
- Soares, M.B., Neto, A.V.C., Zeh, A., Cabral, A.R., Pereira, L.F., do Prado, M.G.B., de Almeida, A.M., Manduca, L.G., da Silva, P.H.M., de Araújo Mabub, R.O. and Schlichta, T.M., 2017. Geology of the Pitangui greenstone belt, Minas Gerais, Brazil: stratigraphy, geochronology and BIF geochemistry. *Precambrian Research*, 291, pp.17-41.
- Stoll, E., Drabon, N. and Lowe, D.R., 2021. Provenance and paleogeography of Archean Fig Tree siliciclastic rocks in the East-Central Barberton Greenstone Belt, South Africa. *Precambrian Research*, 354, p.106041.
- Sylvestre, G., Laure, N.T.E., Djibril, K.N.G., Arlette, D.S., Cyriel, M., Timoléon, N. and Paul, N.J., 2017. A mixed seawater and hydrothermal origin of superior-type banded iron formation (BIF)-hosted Kouambo iron deposit, Palaeoproterozoic Nyong series, Southwestern Cameroon: constraints from petrography and geochemistry. *Ore Geology Reviews*, 80, pp.860-875.
- Tosca, N.J., Guggenheim, S. and Pufahl, P.K., 2016. An authigenic origin for Precambrian greenalite: Implications for iron formation and the chemistry of ancient seawater. *Bulletin*, 128(3-4), pp.511-530.
- Zachariah, J.K., Hanson, G.N. and Rajamani, V., 1995. Postcrystallization disturbance in the neodymium and lead isotope systems of metabasalts from the Ramagiri schist belt, southern India. *Geochimica et Cosmochimica Acta*, 59(15), pp.3189-3203.
- Zegeye, A., Bonneville, S., Benning, L.G., Sturm, A., Fowle, D.A., Jones, C., Canfield, D.E., Ruby, C., MacLean, L.C., Nomosatryo, S. and Crowe, S.A., 2012. Green rust formation controls nutrient availability in

a ferruginous water column. *Geology*, 40(7), pp.599-602.